Cytochrome *c* and Cytochrome *c* Peroxidase Complex As Studied by Resonance Raman Spectroscopy†

Peter Hildebrandt,*,‡ Ann M. English,*,§ and Giulietta Smulevich*,‖

Max-Planck-Institut für Strahlenchemie, Stiftstrasse 34-36, D-4330 Mülheim, FRG, Department of Chemistry and Biochemistry, Concordia University, Montreal, Quebec, Canada H3G 1M8, and Dipartimento di Chimica, Università di Firenze, Via G. Capponi 9, 50121 Firenze, Italy

Received April 4, 1991; Revised Manuscript Received December 9, 1991

ABSTRACT: Complex formation between ferricytochrome *c* peroxidase (CCP) and ferricytochrome *c* from yeast [cyt(Y)] and horse heart [cyt(H)] was studied by resonance Raman spectroscopy. On the basis of a detailed spectral analysis of the free proteins, it was possible to attribute changes in the spectra of the complexes to the individual proteins. At pH 7.0 both cyt(Y) and cyt(H) binding induces an increase in the six-coordinate low-spin configuration of CCP from 9% to 19% at the expense of the five-coordinate high-spin state, which drops from 84% to 74%. In the free and complexed state, CCP exhibits a constant fraction of the six-coordinate high-spin form (~7%). In addition to affecting the coordination state, there is also a cyt-specific structural response of CCP to complexation. In the cyt(Y)–CCP complex, the peripheral vinyl and propionate substituents of CCP are more rigidly fixed in the protein matrix, whereas binding of cyt(H) only slightly perturbs the conformations of these side chains. The biological significance of the conformational changes in CCP are discussed. In contrast to CCP, there are no detectable structural changes in either cyt(Y) or cyt(H) upon complex formation.

Cytochrome *c* peroxidase (CCP)[1] catalyzes the reduction of peroxide by cytochrome *c* (cyt) (Yonetani, 1976). The catalytic cycle starts with the binding of peroxide to the ferric heme iron of CCP, followed by heterolytic cleavage of the O–O bond to give an oxyferryl [Fe(IV)=O] intermediate (compound I). Regeneration of the resting state of CCP is achieved by the transfer of two electrons from ferrocyt molecules.

It is well established that complex formation between cyt and CCP[2] is electrostatically stabilized (Margoliash & Boshard, 1983). Based on the crystal structures of CCP (Finzel et al., 1984) and tuna cyt (Takano & Dickerson, 1980), molecular modeling was used to construct a three-dimensional picture of the 1:1 complex between cyt and CCP by optimizing electrostatic and hydrogen-bonding interactions between the positively charged, lysine-rich domain around the heme crevice of cyt and the negatively charged, aspartate-rich region of CCP (Poulos & Kraut, 1980b; Poulos & Finzel, 1984). Although this model is supported by experimental data from binding studies using chemically modified proteins (Pettigrew, 1978; Waldemeyer et al., 1982; Bisson & Capaldi, 1981), diffraction from cocrystals of cyt(H) and CCP grown at low ionic strength suggests that cyt may possess orientation disorder in the complex (Poulos et al., 1987). Furthermore, a Brownian dynamics simulation of complex formation between the proteins indicates that CCP has a number of possible cyt binding sites (Northrup et al., 1988), a model supported by recent studies on the quenching of fluorescent derivatives of CCP by cyt (Nocek et al., 1991; Hake et al., 1991; Zhang et al., 1990). Thus, while the static model provides information about a possible alignment of the two proteins, two or more 1:1 complexes may exist in solution.

Molecular details of the conformational changes that occur in the proteins upon complex formation also remain to be elucidated. Such data should contribute to our understanding of the catalytic reaction and the control of electron transfer between the hemes. In previous studies, the interaction between cyt(H) and CCP was investigated by NMR and electronic absorption spectroscopy (Gupta & Yonetani, 1973; Erman & Vitello, 1980; Satterlee et al., 1987). Both techniques revealed only subtle spectral changes in the fully oxidized complex compared to the free proteins. In the present work, we employ resonance Raman (RR) spectroscopy, which is more sensitive than absorption spectroscopy to conformational changes in the heme and the heme crevice. In addition, RR offers an advantage over NMR in that dilute concentrations (~10^{-5} M) may be used, and RR has been widely used for conformational studies of CCP and its mutants (Sievers et al., 1979; Rönnberg et al., 1980; Hashimoto et al., 1986; Smulevich et al., 1988, 1990a,b; Dasgupta et al., 1989; Spiro et al., 1990), cyt (Cartling, 1988; Hildebrandt & Stockburger, 1989a,b; Hildebrandt et al., 1990a; Hildebrandt, 1990), and also for protein complexes of cyt (Hildebrandt et al., 1990b; Hildebrandt & Stockburger, 1989b). In this study, we focus on the fully oxidized complex of CCP with cyt from horse heart [cyt(H)] and yeast [cyt(Y)]. Our main goal is to identify conformational changes in the active sites of CCP and cyt that are induced by complex formation between the proteins.

†This research was supported by the Natural Sciences and Engineering Research Council of Canada (A.M.E.), the Italian Consiglio Nazionale delle Ricerche and Ministero dell' Università e della Ricerca Scientifica e Tecnologia (G.S.), and NATO Grant 86/0453 (to G.S. and A.M.E.).

• To whom correspondence should be addressed.
‡ Max-Planck-Institut für Strahlenchemie.
§ Concordia University.
‖ Università di Firenze.

[1] Abbreviations: CCP, cytochrome *c* peroxidase, ferrocytochrome *c*:H_2O_2 oxidoreductase, EC 1.11.1.5; cyt(Y), cytochrome *c* from yeast; cyt(H), cytochrome *c* from horse heart; cyt–CCP, the noncovalent complex between cyt and CCP; 6cLS, six coordinate low spin; 5cHS, five coordinate high spin; 6cHS, six coordinate high spin; RR, resonance Raman.

[2] In the following, the abbreviations "cyt" and "CCP" refer exclusively to the ferric forms of these heme proteins.

0006-2960/92/0431-2384$03.00/0

Materials and Methods

Cytochrome c peroxidase was isolated from *Saccharomyces cerevisiae* and purified as described elsewhere (English et al., 1986; Smulevich et al., 1989). Horse heart (type VI) and yeast (type VIII) cytochromes c were purchased from Sigma and purified by a modified form of the procedure of Brautigan et al. (1978). Prior to use, cyt was converted to the fully oxidized form by addition of a freshly prepared solution of $K_3Fe(CN)_6$. Also, during the RR measurements, the presence of ~ 5 μM $Fe(CN)_6^{3-}$ was essential to avoid the formation of ferrocyt in the laser beam. However, under the conditions of the RR experiments, photodecomposition of $Fe(CN)_6^{3-}$, if it occurred, did not lead to binding of cyanide to the heme iron of cyt or CCP. This was inferred from the absorption spectra measured before and after prolonged laser irradiation of the samples. Furthermore, no time-dependent changes due to laser illumination were detected in the RR spectra.

Complex formation between 15 μM cyt and 15 μM CCP was carried out by mixing solutions of the proteins in 3.3 mM phosphate buffer (pH 7.0). Under these conditions, >90% of the proteins are bound in the complex (Vitello & Erman, 1987; Kornblatt & English, 1986; Erman & Vitello, 1980). RR spectra of the uncomplexed proteins (15 μM) were obtained in 50 mM phosphate buffer (pH 7.0) since the higher phosphate concentration improved the long-term stability of free CCP and had no effect on the RR spectra.

The RR spectra were excited by the 413-nm line of a Kr^+ laser with $\sim$20 mW of power at the sample. The conventional scanning Raman equipment used here has been described in detail elsewhere (Hildebrandt & Stockburger, 1989b). The spectra were recorded with a spectral step width of 0.2 cm^{-1} and a spectral bandwidth of $\sim$2.8 cm^{-1}. Calibration of the double monochromator was carried out after each measurement ($\sim$90 min) using the laser line, which made it possible to limit monochromator drift to $\pm$0.1 cm^{-1}.

All experiments were performed at room temperature using a divided rotating cell (2 × 0.4 mL) which permits the quasisimultaneous measurement of two different samples (Rousseau, 1981; Hildebrandt & Stockburger, 1989b). In a series of measurements, RR spectra of cyt, CCP, and the cyt–CCP complex were recorded in each of the three possible pairwise combinations (cyt + CCP, cyt + cyt–CCP, CCP + cyt–CCP). Thus, two spectra were obtained for each sample in different combinations, and only duplicate spectra whose difference spectrum yielded a straight line were averaged (Hildebrandt et al., 1990b). To obtain a good signal-to-noise ratio, it was necessary to repeat this procedure several times so that about four spectra were averaged for each sample, and fresh solutions were used after exposure of the proteins to the laser beam for $\sim$2 h. This procedure also allowed the relative RR band intensities of cyt and CCP to be directly compared because the attenuation of the exciting laser beam is the same in the cyt and CCP solutions since both proteins have an extinction coefficient of $\sim$96 mM^{-1} cm^{-1} at 413 nm. The optical density of the 1:1 cyt–CCP complex is twice that for the single components at this wavelength so attenuation of the laser beam had to be taken into account. The RR intensities of the cyt–CCP spectra were normalized with respect to the spectra of the uncomplexed proteins by multiplying by a Beer's law factor of 1.6. RR spectra of 1:1 mixtures of cyt and CCP were obtained by adding the spectra of the individual components. As shown previously, this procedure is equivalent to the direct measurement of the spectrum of a physical mixture of both proteins at high ionic strength (Hildebrandt et al., 1990b). The background was removed from all spectra displayed in this work by polynomial subtraction. The spectra so obtained were analyzed by a band-fitting program using Lorentzian line shapes, which have been found to best describe the measured band profiles of hemes and other chromophores in proteins (Alshuth & Stockburger, 1986; Hildebrandt & Stockburger, 1989a,b; Hildebrandt et al., 1989, 1990a,b; Morikis et al., 1991).

Results

Spectral Changes upon Complex Formation. RR spectra of the cyt(H)–CCP and cyt(Y)–CCP complexes were investigated over the entire range of the fundamental vibrations (200–1700 cm^{-1}). To identify regions of spectral change upon complex formation, the RR spectra of both cyt and CCP were subtracted from those of the complexes, and a number of peaks were observed between 1450–1650 cm^{-1} and 300–500 cm^{-1} in the difference spectra. These two regions of the RR spectrum include vibrations which provide complementary structural information. Above 1450 cm^{-1}, the frequencies of most of the RR bands can be correlated with the core size of the porphyrin and, hence, with the spin and coordination state of the heme iron (spin marker bands) (Parthasarathi et al., 1987; Kitagawa & Ozaki, 1987; Spiro & Li, 1988). The bands below 500 cm^{-1} originate from modes which, to a significant degree, include vibrations associated with the peripheral substituents of the porphyrin, so that these modes yield insight into the molecular details of heme–protein interactions (fingerprint region) (Choi & Spiro, 1983; Hildebrandt, 1990).

Since most of the RR bands of cyt and CCP strongly overlap and exhibit similar RR cross sections on 413-nm excitation, the difference spectra cannot be interpreted without a detailed analysis of the RR spectra of the uncomplexed proteins. This analysis was restricted to the spin marker and fingerprint regions, but it should be mentioned that spectral differences were also noted in other parts of the RR spectra (ν_4 $\sim$1370 cm^{-1}; ν_7 $\sim$670–700 cm^{-1}).

Analysis of the RR Spectra of the Uncomplexed Proteins. (A) Spin Marker Band Region. The analysis of the RR spectra of cyt(H) and cyt(Y) in this region is straightforward since both species exist exclusively in the six-coordinate low-spin (6cLS) configuration and exhibit relatively sharp peaks with little overlap (Figure 1). The bands can be readily assigned following the notation of Abe et al. (1978), and the results are listed in Table I. Notable are the bands at 1596.0 and 1594.7 cm^{-1} in cyt(Y) and cyt(H), respectively, which are assigned to the E_u mode, ν_{37}, since no other porphyrin fundamental is expected in this region (Parthasarathi et al., 1987). As suggested previously (Valance & Strekas, 1982; Hildebrandt, 1990), RR activation of these modes, which are RR-forbidden under D_{4h} symmetry, indicates a symmetry lowering of the heme. In fact, the crystal structure of cyt(H) reveals that the heme is saddle shaped rather than planar (Bushnell et al., 1990), and this structural peculiarity may also account for deviations of some of the marker band frequencies from the values expected for 6cLS ferric heme (Hildebrandt, 1990).

A comparison of the RR spectra of cyt(Y) and cyt(H) reveals small differences in the spin marker band region (Table I). The bands of cyt(Y) are broader that those of cyt(H) with the exception of ν_{38}. In addition, differences in relative intensities (notably ν_{11}, ν_2, and ν_{10}) and frequencies (notably ν_{38}) are revealed from the data in Table I.

In contrast to cyt, the five-coordinate high-spin (5cHS) state prevails in CCP at pH 7 (Yonetani & Anni, 1987; Smulevich et al., 1988, 1989). The ν_3 mode for this configuration is expected at $\sim$1490 cm^{-1} (Parthasarathi et al., 1987; Smulevich et al., 1988). However, attempts to fit the relatively strong

Table I: Spectral Parameters of Cytochrome *c*[a]

	cyt(Y)						cyt(H)					
	uncomplexed			CCP complex			uncomplexed			CCP complex		
mode	ν_i	$\Delta\nu_i$	I_i	ν_i	$\Delta\nu_i$	I_i	ν_i	$\Delta\nu_i$	I_i	ν_i	$\Delta\nu_i$	I_i
spin marker band region												
ν_3	1501.1	10.1	1010	1500.7	10.0	758	1500.4	9.9	990	1500.0	9.0	653
ν_{38}	1538.8	9.0	45	1539.5	8.2	67	1547.4	13.4	76	1547.5	13.5	158
ν_{11}	1557.1	15.8	278	1558.6	14.8	237	1558.7	9.3	178	1559.7	14.9	446
ν_2	1582.7	13.9	1639	1582.9	14.2	1776	1582.0	13.0	1017	1581.9	14.8	1527
ν_{37}	1596.0	16.2	415	1591.4	15.3	211	1594.7	15.3	457	1593.5	15.2	298
	1629.1	12.1	81									
ν_{10}	1634.1	9.8	503	1634.2	10.0	468	1633.3	8.6	574	1633.5	8.5	428
fingerprint region												
ν_8	349.2	11.5	2921	349.7	10.9	2769	348.9	9.3	3502	349.0	9.1	3427
pyr tilt	361.2	10.3	958	361.3	9.9	882	361.9	9.2	1119	361.8	9.9	1192
$2\nu_{35}$	375.1	7.3	294	375.1	7.6	277	374.5	6.1	324	374.1	7.0	405
	381.9	8.1	390	381.5	8.0	384	381.9	6.6	471	381.6	7.0	529
$\nu_{34} + \nu_{35}$	398.1	10.6	1450	397.8	10.2	1508	397.9	8.4	1806	398.0	8.7	2004
$2\nu_{34}$	413.1	9.1	1155	412.7	9.0	1012	413.0	7.5	1255	412.9	8.0	1358
	419.3	7.8	574	420.1	8.0	532	419.0	6.6	609	418.7	6.8	711
prop bend	442.4	7.9	192	441.5	9.2	184	446.1	12.6	633	445.9	12.9	782
	449.7	13.5	194	450.2	13.7	248						

[a] Frequencies (ν_3) and half-widths ($\Delta\nu_i$) are given in cm^{-1}. The integrated band intensities (I_i; arbitrary units) are at different scales in the spin marker and fingerprint regions, and I_i for the CCP complexes were normalized with respect to I_i for cyt by multiplication by 1.6 (see text). The assignment of the bands is discussed in the text.

Table II: Spectral Parameters of CCP[a]

	uncomplexed			cyt(H) complex			cyt(Y) complex		
mode	ν_i	$\Delta\nu_i$	I_i	ν_i	$\Delta\nu_i$	I_i	ν_i	$\Delta\nu_i$	I_i
spin marker band region									
ν_3 6cHS	1485.1	13.0	168	1485.3	12.5	195	1485.4	13.1	172
ν_3 5cHS	1492.4	13.2	1163	1492.2	12.9	1007	1492.3	13.2	1043
ν_3 6cLS	1503.1	8.7	77	1503.3	8.0	142	1503.6	8.2	166
ν_{38} 5cHS	1525.7	10.2	143	1525.1	9.1	102	1526.1	8.9	117
ν_{11} 5cHS	1548.1	15.0	728	1548.2	15.1	586	1548.3	14.8	638
ν_2 6cHS	1563.2	9.8	449	1564.4	10.6	371	1563.3	10.0	484
ν_2 5cHS	1570.3	13.9	2034	1570.0	13.3	1587	1570.2	13.9	1790
ν_{37} 5cHS	1585.9	12.1	449	1586.8	11.0	314	1586.5	12.2	401
ν_{10} 6cHS	1616.1	7.2	303	1615.7	6.8	298	1616.0	7.3	318
$\nu_{C=C}$ (1)	1620.4	7.6	121	1620.3	7.2	85	1619.8	7.0	120
ν_{10} 5cHS and $\nu_{C=C}$ (2)	1628.2	15.1	809	1628.6	14.4	694	1628.5	15.4	727
fingerprint region									
	327.6	10.7	196	327.8	10.1	157	328.3	11.3	220
6cHS/5cHS	336.0	12.6	893	335.9	12.7	902	335.8	12.5	888
6cLS	345.2	8.8	356	345.7	8.9	373	345.7	8.9	368
5cHS	350.1	8.4	536	349.9	8.2	425	350.1	8.0	470
5cHS	374.0	10.0	756	373.9	10.2	670	374.0	10.0	631
6cLS/6cHS	381.3	12.0	134	380.1	11.1	133	380.9	11.7	128
5cHS	403.6	11.8	1036	403.7	11.9	921	403.6	12.0	862
$\delta C_B C_\alpha C_\beta$	412.4	11.9	170	412.2	12.7	213	412.5	11.6	209
$\delta C_B C_\alpha C_\beta$	422.2	12.5	100	422.0	11.1	86	422.8	9.8	105
prop bend	439.2	12.8	215	438.9	13.0	218	438.4	11.2	264

[a] Frequencies (ν_3) and half widths ($\Delta\nu_i$) are given in cm^{-1}. The integrated band intensities (I_i; arbitrary units) are at different scales in the spin marker and fingerprint regions, and I_i for the cyt complexes were normalized with respect to I_i for CCP by multiplication by 1.6 (see text). The assignment of the bands is discussed in the text.

band in this region by a single Lorentzian curve at 1492.4 cm^{-1} failed. The band fitting analysis clearly revealed two minor components at 1485.1 and 1503.1 cm^{-1}. These bands correspond to six-coordinate high-spin (6cHS) and 6cLS configurations, respectively. The presence of these configurations in addition to the dominant 5cHS form is also reflected in the ν_2 region, where two bands at 1570.3 (5cHS) and 1563.2 cm^{-1} (6cHS) are found. The corresponding 6cLS mode, expected at ~1580 cm^{-1}, strongly overlaps the 5cHS ν_{37} mode, so these two modes probably contribute to the rather broad Lorentzian band at 1585.9 cm^{-1}. On the basis of the intensity ratio of the ν_3 and ν_2 modes of 6cLS CCP measured at pH >9 (Smulevich et al., 1988), the contribution of the 6cLS ν_2 mode to the 1585.9-cm^{-1} band is estimated to be <25%, hence its intensity would be only ~5% that of the adjacent strong 1570.3-cm^{-1} band. Since the frequencies and half-widths of neither the ν_2 (6cLS) mode nor the ν_{37} (5cHS) mode are known, resolution of the 1585.9-cm^{-1} peak into two components would not yield physically meaningful results.

The vibration pattern of the RR spectrum of CCP between 1600 and 1650 cm^{-1} is also rather complex. In this region, the porphyrin ν_{10} modes and the vinyl stretching vibrations are expected. The band at 1628.2 cm^{-1} is assigned to the 5cHS ν_{10} mode, but the corresponding 6cLS mode expected at ~1638 cm^{-1} was not detected. This may be due to the low intensity of this band, which is much weaker than the 6cLS ν_3 on Soret excitation (Smulevich et al., 1988). The 1616.1-cm^{-1} band, which is higher in intensity than the 6cHS ν_3 mode at 1485.1 cm^{-1} (Table II), is attributed to the 6cHS ν_{10} mode, since a strong band at this position is also observed in the RR spectra of the 6cHS Phe-51 mutant of CCP (Smulevich et al., 1988). The 1620.4-cm^{-1} band is readily assigned to the vinyl

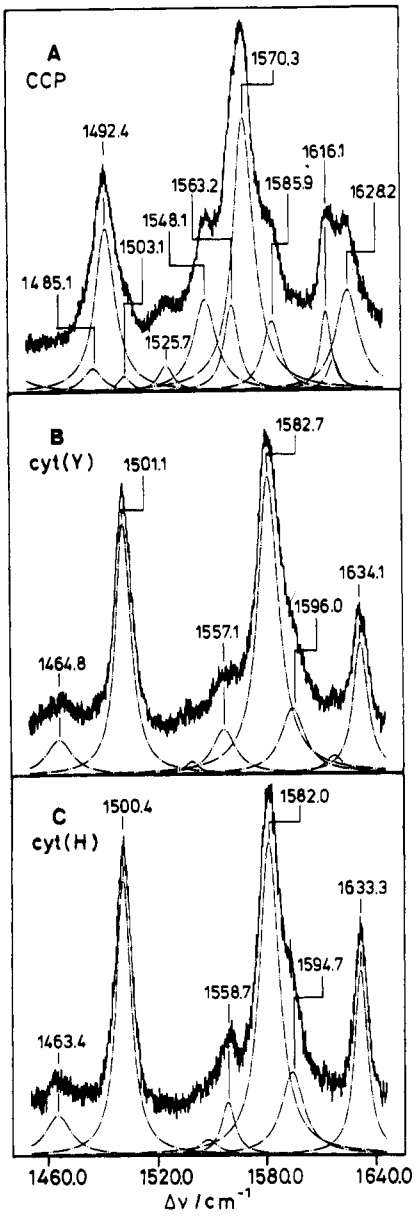

FIGURE 1: RR spectra of (A) CCP, (B) cyt(Y), and (C) cyt(H) in the spin marker region excited at 413 nm. The broken lines represent the fitted Lorentzian curves.

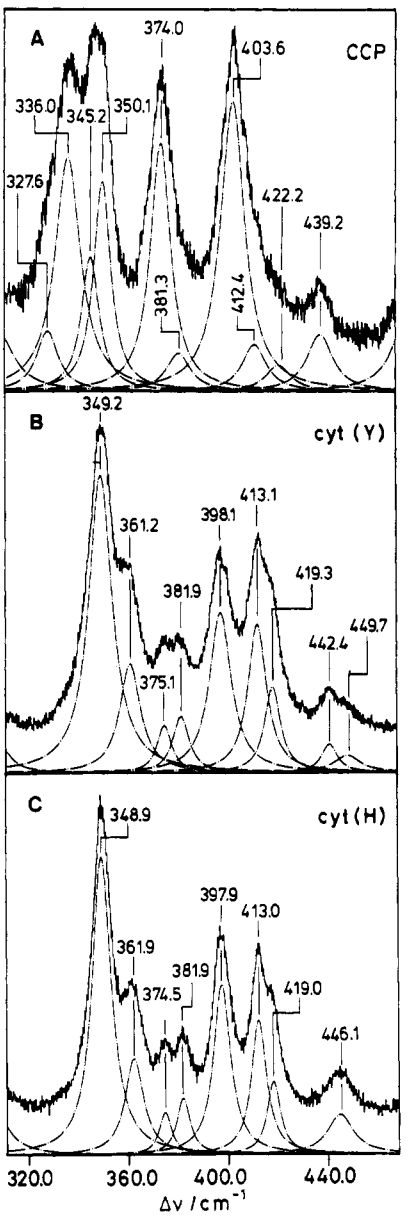

FIGURE 2: RR spectra of (A) CCP, (B) cyt(Y), and (C) cyt(H) in the fingerprint region excited at 413 nm. The broken lines represent the fitted Lorentzian curves.

stretching vibration, and the narrow half-width of 7.6 cm^{-1} indicates that inhomogeneous broadening is small. This raises some doubt that this band originates from both substituents, since it would imply that the two vinyl groups exhibit identical conformations. More likely, a second vinyl stretching vibration is hidden under the unusually broad (half-width 15.1 cm^{-1}) 1628.2-cm^{-1} band. Support for this comes from previous RR studies where a band, which can be tentatively assigned to the second vinyl stretching mode, is observed at 1628 cm^{-1} in the high pH spectra of 6cLS CCP mutants (Smulevich et al., 1988, 1991). Again, as in the case of the 1585.9-cm^{-1} band, reliable deconvolution of the 1628.2-cm^{-1} band is not possible. The remaining bands in the RR spectrum of CCP can be attributed exclusively to the marker bands of the 5cHS form (Table II).

Analysis of the RR Spectra of the Uncomplexed Proteins. (B) Fingerprint Region. In previous studies, the low-frequency region of the RR spectrum of cyt(H) was analyzed in detail (Hildebrandt et al., 1990a; Hildebrandt, 1990), and a preliminary assignment, which is also adopted in this work (Table I), will be presented elsewhere. The vibrational pattern in this region is a characteristic signature of the specific structure of the heme pocket (Hildebrandt, 1990), and the far reaching similarities in the RR spectra of cyt(H) and cyt(Y) (Figure 2) reflect the close structural homology of both proteins. The most pronounced difference between the spectra is in the region at ~440 cm^{-1}. The 446.1-cm^{-1} band of cyt(H) was attributed to a propionate bending vibration (Hildebrandt, 1990), and a recent normal mode analysis supports this assignment (L. L. Gladkov, personal communication). In cyt(Y) this band splits into two components pointing to different conformations or hydrogen-bonding interactions of the two propionate groups. Furthermore, one notes a significant broadening of all the bands in the fingerprint region of cyt(Y) compared to cyt(H) (Table I).

In the analysis of the fingerprint region of the CCP spectrum, interference by various spin and coordination states is again encountered. Since the spectral parameters of the individual species are not known, band fitting was carried out using the minimum number of Lorentzian curves required to obtain a good fit. This does not necessarily imply that each calculated curve represents a pure vibrational band. Nonetheless, in most cases it is possible to identify the major con-

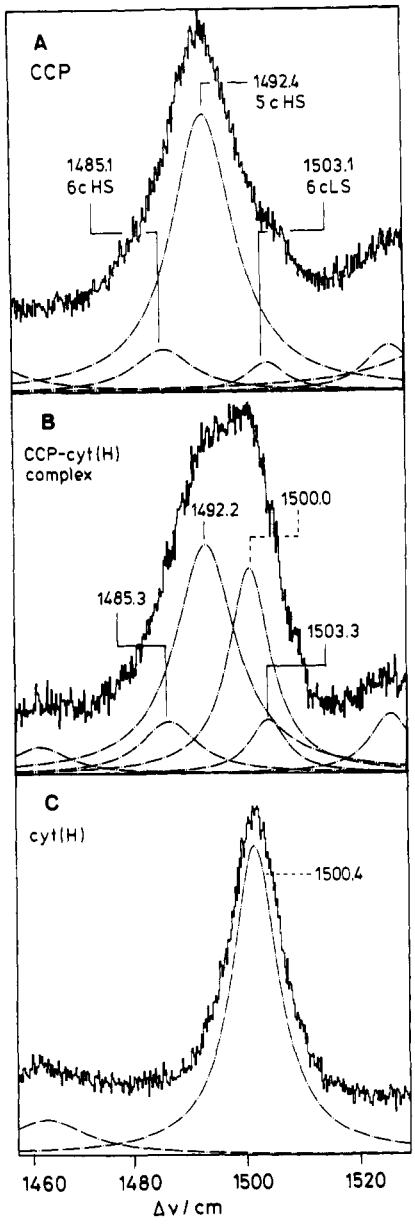

FIGURE 3: RR spectra of (A) CCP, (C) cyt(H), and (B) the 1:1 complex of both proteins in the ν_3 region excited at 413 nm. The Lorentzian curves labeled by solid and dashed lines refer to CCP and cyt(H), respectively.

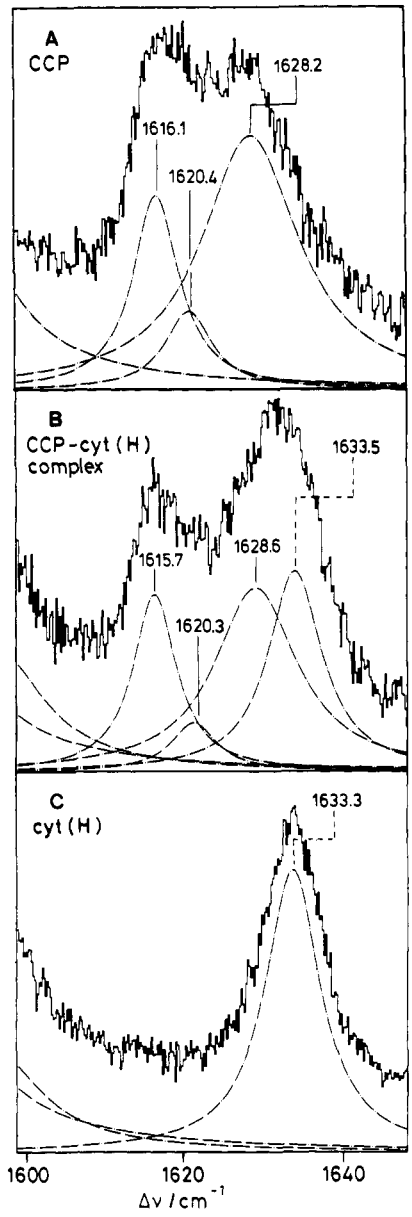

FIGURE 4: RR spectra of (A) CCP, (C) cyt(H), and (B) the 1:1 complex of both proteins in the ν_{10} region excited at 413 nm. The Lorentzian curves labeled by solid and dashed lines refer to CCP and cyt(H), respectively.

tributions to these curves on the basis of the RR bands observed for CCP mutants at different pH's (Smulevich et al., 1988). Hence, the dominant bands at 350.1, 374.0, and 403.6 cm^{-1} are attributed to the 5cHS configuration (Table II). The 336.0-cm^{-1} band may include contributions from both HS species, since this band appears to be present in both 5cHS and 6cHS CCP mutants, whereas the 345.2-cm^{-1} band probably results from the 6cLS state, and the 381.3-cm^{-1} band appears to have contributions from both 6cHS and 6cLS states. According to Uchida et al. (1988), b-type hemes show two RR bands between 410 and 440 cm^{-1} that originate from coupled pyrrole and vinyl bending vibrations ($\delta C_B C_\alpha C_\beta$). In CCP, the bands at 412.4 and 422.2 cm^{-1} are attributed to these modes, while the propionate bending vibration is tentatively assigned to the 439.2-cm^{-1} band analogous to the RR assignment for cyt. Table II summarizes our assignments for CCP.

Analysis of the RR Spectra of the Cyt–CCP Complexes. (A) Spin Marker Band Region. The band fitting of these spectra followed the protocol developed in a previous study on the cyt(H)–cytochrome *c* oxidase complex and cyt(H) bound to phospholipid vesicles (Hildebrandt et al., 1990a,b). In brief, the spectral parameters (relative band intensities, half-widths, and frequencies) of the individual components were used to generate the RR spectra of the cyt–CCP complexes. Then the spectral parameters were released stepwise by progressively lowering the damping constant, and, as for the free proteins, the standard deviations of the final fits were just within the noise level of the RR spectra. Figure 3 shows the results of such an analysis for the ν_3 band region of cyt(H)–CCP. It can be seen immediately that the intensity distribution among the ν_3 marker bands is considerably different in free and complexed CCP. Relative to the 1485-cm^{-1} band (6cHS), a distinct increase in the 1503-cm^{-1} band (6cLS) at the expense of the 1492-cm^{-1} band (5cHS) is noted for the complex. The region above 1600 cm^{-1} (Figure 4) offers a similar picture since the intensity ratio of the 1628- (ν_{10}, 5cHS) and 1616-cm^{-1} (ν_{10}, 6cHS) bands is also lower in the complex compared to that in free CCP. Comparable intensity changes are also observed in the ν_2 band region, particularly for the cyt(Y)–CCP complex (1563 vs 1570 cm^{-1}; Table II). At-

Table III: Relative Concentrations (c_i) of the Various Spin and Coordination States of CCP[a]

	5cHS	6cLS	6cHS
uncomplexed CCP	0.84	0.09	0.07
cyt(Y)–CCP	0.73	0.20	0.07
cyt(H)–CCP	0.74	0.18	0.08

[a] The relative concentrations (c_i) were determined from the integrated band intensities (I_i) in Table II according to Hildebrandt et al. (1990a). The average standard deviation for the c_{5cHS} in uncomplexed CCP and the cyt–CCP complexes was 3.2%. For the corresponding c_{6cLS} and c_{6cHS} values, the standard deviation was estimated to about 5%.

tempts to fit the RR spectra of the cyt–CCP complexes using the spin-state distribution of free CCP led to ~20% increase in the standard deviation of the fits.

Both cyt(Y) and cyt(H) complexation gives rise to similar changes in the CCP band intensities, which points to a shift in the coordination equilibrium of CCP on binding cyt. An inspection of the integrated band intensities (I_i) listed in Table II reveals that the intensities of the 5cHS marker bands decrease by an average of ~15%, while ν_3 of the 6cLS form (which is the only band that can be unambiguously attributed to the 6cLS state) increases by a factor of ~2. On the other hand, the average intensity of the 6cHS marker bands remains largely constant in free and complexed CCP. The integrated RR band intensities in Table II for the different configurations (5cHS, 6cLS, and 6cHS) can be converted to relative concentrations, c_i, following the procedure described by Hildebrandt et al. (1990a). The following expression holds for each normal mode of any given CCP species:

$$c_i = F_i I_i \quad (1)$$

The proportionality constants F_i can be determined from

$$1 = F_{5cHS}I_{a,5cHS} + F_{6cLS}I_{a,6cLS} + F_{6cHS}I_{a,6cHS} \quad (2a)$$

$$1 = F_{5cHS}I_{b,5cHS} + F_{6cLS}I_{b,6cLS} + F_{6cHS}I_{b,6cHS} \quad (2b)$$

$$1 = F_{5cHS}I_{c,5cHS} + F_{6cLS}I_{c,6cLS} + F_{6cHS}I_{c,6cHS} \quad (2c)$$

The indices a, b, and c refer to the intensities obtained from the the RR experiments for free CCP, cyt(H)–CCP, and cyt(Y)–CCP, respectively. Thus, the F_i constants were determined for each normal mode in the spin marker band region using eq 2a–c, and the corresponding c_i values (eq 1) were averaged and are listed in Table III.

The underlying assumption of this approach is that the F_i factors are the same in free and complexed CCP. Alternatively, the RR intensity changes could be attributed to perturbation of the electronic transitions of the different coordination states. However, this is unlikely since it would imply, for example, that the resonance enhancement of the ν_3 mode of the 6cLS species is increased by a factor of ~2 on cyt–CCP complexation. Unlike the significant intensity changes, complex formation induces only small frequency shifts in the marker bands of CCP (Table II). Intensity changes and small frequency shifts were also observed for the spin marker bands of both cyt(H) and cyt(Y) on complexation (Table I), and these are consistent with a conformational change in cyt as discussed below.

Analysis of the RR Spectra of the Cyt–CCP Complexes. (B) Fingerprint Region. Analysis of the low-frequency region by the above procedure is more complicated due to the larger number of overlapping bands (Figure 5). For example, cyt and CCP bands at ~413, 374, and 350 cm^{-1} accidentally coincide to within ±1 cm^{-1}, so their intensities cannot be determined accurately and the results must be interpreted with caution. Nonetheless, the intensity of the 403-cm^{-1} band of 5cHS CCP is significantly lower in both cyt(Y)–CCP (Figure 5) and cyt(H)–CCP than in free CCP, which mirrors the intensity behavior observed for the spin marker bands of 5cHS CCP (Table II).

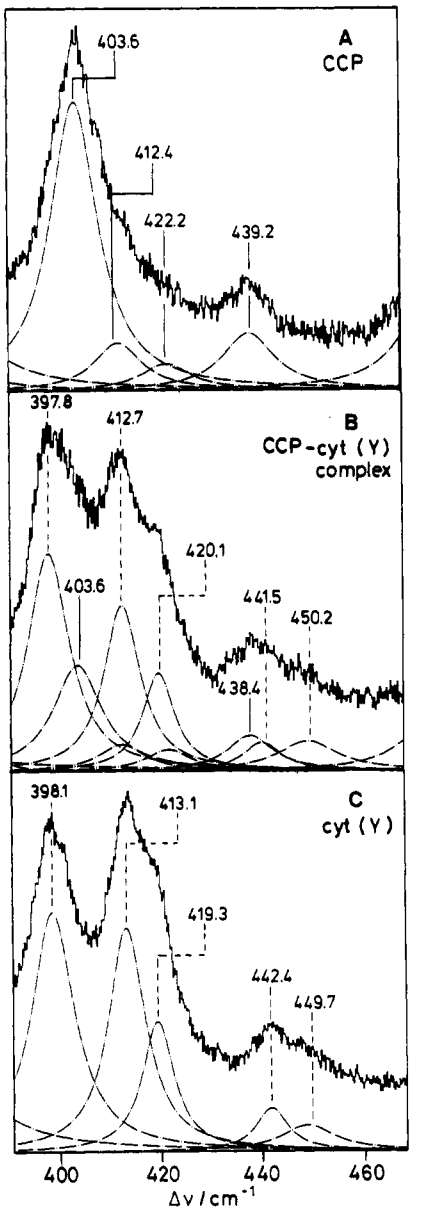

FIGURE 5: RR spectra of (A) CCP, (C) cyt(Y), and (B) the 1:1 complex of both proteins in the fingerprint region excited at 413 nm. The Lorentzian curves labeled by solid and dashed lines refer to CCP and cyt(Y), respectively.

The cyt(Y)–CCP bands above 420 cm^{-1} show distinct changes in frequency and half-width compared to those of free CCP and cyt(Y). More precisely, the cyt(Y) band at 441.5 cm^{-1} is broadened by 1.3 cm^{-1}, while the CCP bands at 422.8 and 438.4 cm^{-1} are narrower by 2.7 and 1.6 cm^{-1}, respectively, in the complex. This is quite a contrast to the cyt(H)–CCP complex, in which only the vinyl bending at 422.0 cm^{-1} exhibits a smaller (1.4 cm^{-1}) bandwidth. On the other hand, the intensities of the cyt(H) and cyt(Y) propionate bending vibrations at 445.9 and 450.2 cm^{-1}, respectively, are considerably enhanced on complexation (Table I).

Discussion

Conformations of the Uncomplexed Proteins. (A) Cytochromes c. High-resolution crystal structures are available

for ferrocyt(Y) (Louie et al., 1988; Louie & Brayer, 1990) and for cyt(H) (Bushnell et al., 1990). The overall similarities in the structures are in line with the RR spectroscopic results which reveal far-reaching similarities between cyt(Y) and cyt(H). Nevertheless, there are some distinct spectral differences between the two cyts which reflect conformational deviations. These may be beyond the resolution of the crystal structure or due to conformations accessible to the proteins only in solution. For example, the broader RR bands observed for cyt(Y) compared to cyt(H) (Table I) indicate substantially higher flexibility of the heme in the yeast protein matrix. This suggests that the steric constraints on the heme, imposed by adjacent amino acid side chains, are more relaxed in cyt(Y) than in cyt(H), which may also account for the different intensity distribution between the 375- and 382-cm^{-1} bands in the two proteins. These bands were previously assigned to porphyrin vibrations in two heme rotational isomers that presumably arise due to restricted rotational mobility of the peripheral substituents (Hildebrandt, 1990). If this assignment is correct, then the relative intensities of the bands would suggest that the populations of the two rotational isomers are apparently different in cyt(Y) and cyt(H).

The most pronounced difference in the conformation of the cyt heme, detectable from the RR spectra, is associated with the propionate side chains, since the 446-cm^{-1} band of cyt(H) splits into two components in cyt(Y). On the basis of a comparison of the crystal structures, Bushnell et al. (1990) pointed out that structural differences between cyt(Y) and cyt(H) are localized around residues 56 and 57, and similar conclusions can be drawn from the comparative NMR study of cyt(Y) and cyt(H) in solution (Gao et al., 1990). These differences originate from the replacement of Ile-57 by Val in cyt(Y) (Louie et al., 1988; Louie & Brayer, 1990), and this modifies the environment of Trp-59 which is hydrogen bonded to propionate-7. We tentatively assign the 442.4-cm^{-1} band to the bending vibration of propionate-7, since its small bandwidth (7.9 vs 13.2 cm^{-1} for the component at 449.7 cm^{-1}) could arise from the more compact structure of cyt(Y) in this region (Louie & Brayer, 1990: Bushnell et al., 1990).

Cyt(Y) exhibits higher frequencies than cyt(H) for all the well-resolved spin marker bands (Figure 1). These shifts point to a slightly smaller heme core size (Parthasarathi et al., 1987) in the yeast protein, which could be induced by a conformational change of one of the axial ligands (e.g., in a bond angle). The striking differences in the relative intensities of the marker bands of the two cyts may result from subtle differences in the Soret transitions which delicately control the resonance enhancement of the various vibrational modes.

Conformations of the Uncomplexed Proteins. (B) Cytochrome c Peroxidase. At pH 7, free CCP is predominantly 5cHS (Table III). The iron atom is displaced by ~0.2 Å out of the heme plane toward its axial ligand, the proximal His-175 (Poulos et al., 1980; Finzel et al., 1984). This ligand also serves as a proton donor to Asp-235, which is part of an extended hydrogen-bonding network on the proximal side of the heme pocket. The involvement of His-175 in hydrogen bonding, and its resultant high basicity, should serve to constrain the movement of the iron into the heme plane and to lower its affinity for a sixth ligand, which would account for the high stability of the 5cHS configuration over a wide pH range (Smulevich et al., 1988, Yonetani & Anni, 1987). The importance of the proximal hydrogen-bonding network in maintaining the 5cHS state of CCP is clearly seen on Asp-235 → Asn replacement. In the Asn-235 mutant, the iron moves into the heme plane and interacts strongly with the distal water molecule (wat-595), which is 2.0 Å from the heme in this mutant (Wang et al., 1990). This accounts for the fact that Asn-235 is already 6cLS at pH 6 (Smulevich et al., 1988).

Wat-595 is also a plausible candidate for the distal axial ligand in the 6c states of wild-type CCP, since it appears at 2.4 Å above the heme plane in the X-ray structure (Poulos et al., 1980; Finzel et al., 1984). Binding of wat-595 to the Fe would account for the 7% 6cHS CCP observed at pH 7 (Table III). Although water is a weak ligand, the basicity of His-175 may increase the ligand-field strength enough to populate 9% of the 6cLS state (Table III), or deprotonation of the iron-bound water molecule may be facilitated by the polar distal heme pocket (Poulos et al., 1980; Finzel et al., 1984), so that hydroxide is formed as a strong-field ligand at pH 7 (Smulevich et al., 1988). Alternatively, the sixth ligand in the 6cLS state may be the imidazole of the distal His-52 which coordinates to CCP at high pH (Smulevich et al., 1991).

Structural Changes upon Complex Formation. (A) Cytochrome c Peroxidase. Optimization of electrostatic and hydrogen-bonding interactions in the construction of the cyt–CCP model complex required structural changes in CCP, the most important being a reorientation of His-181 (Poulos & Kraut, 1980b; Poulos & Finzel, 1984). Since this residue is hydrogen bonded to propionate-7, which in turn is linked to Arg-48 via a water molecule, cyt-induced repositioning of His-181 would perturb hydrogen-bonding interactions in the distal heme pocket of CCP. Considering the crucial role of Arg-48 in the binding of distal ligands (Smulevich et al., 1988, Edwards & Poulos, 1990), alteration of its hydrogen-bonding network may increase the amount of 6cLS CCP observed in the complex (Table III). In fact, the importance of the distal hydrogen-bonding network is apparent from RR studies on the Gly-181 mutant of CCP. This mutant, which has lost the hydrogen-bonding capability of His-181, is 6cLS even at pH 7 (Smulevich et al., 1991). Hence, consistent with the view that His-181 is repositioned in the cyt–CCP complex, the most pronounced structural change in CCP detectable by RR upon complex formation is the redistribution of the heme between 6cLS and 5cHS configurations (Table III). In contrast, the percent 6cHS heme is not affected upon cyt binding. This raises some doubt that 6cLS and 6cHS states are in equilibrium at room temperature (Smulevich et al., 1990a) and suggests that the 7% 6cHS heme in free and complexed CCP is more likely due to the presence of a small amount of aged CCP in our preparations (Smulevich et al., 1989).

The observed coordination-state changes in CCP are quantitatively the same on cyt(H) and cyt(Y) binding (Table III). However, there are also cyt-specific conformational responses of CCP to complexation. The distinct narrowing of the bands assigned to the vinyl and propionate bending vibrations of CCP on cyt(Y) binding suggests that these substituents are more rigidly fixed in cyt(Y)–CCP compared to either cyt(H)–CCP or free CCP. In particular, the decrease in both frequency and bandwidth of the propionate bending vibration at 439.2 cm^{-1} supports the view that cyt(Y) binding perturbs the hydrogen-bonding network involving His-181, Arg-48, and propionate-7. On the other hand, in cyt(H)–CCP only the vinyl bending vibration at 422.0 cm^{-1} exhibits a decrease in inhomogeneous broadening, and even this is less than that observed for cyt(Y)–CCP. Apparently, structural details in the binding domains of cyt(H) and cyt(Y) exert a different influence on the heme environment of CCP. Remarkably, this is detectable even in the vinyl region of the CCP heme pocket which is remote from the cyt binding domain. Recent computer modeling results show a number of differences between

the CCP complexes of cyt(Y) and tuna cyt (Lum et al., 1987). In particular, the interfacial contact distance between His-181 of CCP and Phe-82 of cyt is 3.3 Å shorter in the cyt(Y)–CCP complex than in the tuna cyt–CCP complex. Similar differences between the cyt(Y)–CCP and cyt(H)–CCP complexes may give rise to the variations observed here in their RR spectra.

Structural Changes upon Complex Formation. (B) Cytochromes c. In previous studies, it was found that binding of cyt(H) in a variety of nonphysiological and physiological complexes induces a conformational equilibrium between two states (I and II) (Hildebrandt & Stockburger, 1989a,b; Hildebrandt et al., 1990a,b; Hildebrandt, 1990). In state I, the heme structure of native cyt(H) is fully preserved, while in state II the heme crevice opens and the iron–Met-80 bond is weakened, leading to an equilibrium between 6cLS and 5cHS configurations. In the complex with cytochrome *c* oxidase (Hildebrandt et al., 1990b), it was assumed that opening of the heme cleft of cyt(H) is initiated by the rupture of the intramolecular Lys-13–Glu-90 salt bridge due to the involvement of Lys-13 in intermolecular salt bridge formation. This lysine residue most probably participates in intermolecular electrostatic interactions also in the cyt–CCP complex (Poulos & Kraut, 1980b; Poulos & Finzel, 1984; Northrup et al., 1988), so that similar conformational changes might be expected.

The RR spectra of both states I and II of cyt(H) can be easily distinguished from each other and from that of the uncomplexed species (Hildebrandt & Stockburger, 1989a; Hildebrandt et al., 1990a). The fingerprint and marker band regions of the RR spectrum of cyt(H)–CCP show no indication of state II. For example, ν_2 and ν_{10} shift by 6 and 4 cm^{-1}, respectively, to 1588 and 1637 cm^{-1} in state II (6cLS), but no bands are present at these positions in the RR spectrum of cyt(H)–CCP. Furthermore, an unique feature of both 6cLS and 5cHS state II is that the propionate bending vibration at 446 cm^{-1} vanishes, whereas the RR intensity of this mode relative to the 413-cm^{-1} mode is ~15% higher in cyt(H)–CCP than in free cyt(H) (Table I). Even more pronounced changes are noted in the spin marker band region where the intensity ratios ν_3/ν_2 and ν_{10}/ν_2 drop by a factor of ~2.2 in the cyt(H)–CCP complex relative to free cyt(H) (Table I). In fact, these intensity changes agree very well with the corresponding changes observed for state I formed upon cyt(H) binding to negatively charged phospholipid bilayers (Hildebrandt et al., 1990a). Also, the small frequency shifts observed for some of the cyt(H) modes on CCP complexation bring them closer to the state I frequencies; thus, these observations imply that binding of cyt(H) to CCP stabilizes state I. Spectral differences between state I and the uncomplexed cyt(H) may be due either to subtle conformational perturbations on complexation or to a Stark effect on the electronic and vibrational energy levels of the cyt heme due to the electric field of CCP (Hildebrandt & Stockburger, 1989a). It is not known if cyt(Y) undergoes conformational equilibria similar to cyt(H) since its complexation has not been studied previously by RR spectroscopy. However, on binding to CCP, the intensity ratios ν_3/ν_2 and ν_{10}/ν_2 drop by a factor of only ~1.3 in cyt(Y). The difference in spectral response to complexation suggests variation in the CCP binding regions of the two cyts, consistent with the results from fluorescence quenching studies (Nocek et al., 1991).

Biological Implications. In the first step of the catalytic cycle of CCP, peroxide binds to the vacant coordination site of the heme iron (Poulos & Kraut, 1980a). Binding of a sixth ligand requires movement of the iron into the heme plane, and the present results demonstrate that this is facilitated upon cyt complexation. However, the cyt-induced 6cLS state must be different from the aging-induced 6c states reported for CCP since the latter inhibit peroxide binding (Balny et al., 1987), whereas the rate of peroxide binding to free and complexed CCP is essentially the same (Hoth & Erman, 1984). Also, since the Fe(IV)=O heme of CCP is 6c, maintaining the Fe atom close to the heme plane would serve to lower the heme reorganizational energy on reduction to the 5cHS heme of the resting enzyme.

Functionally relevant structural changes in cyt itself are not required prior to CCP compound I formation. In fact, formation of state II of cyt, as in the cytochrome *c* oxidase complex (Hildebrandt et al., 1990b), may even inhibit peroxide degradation. Since opening of the heme crevice in state II is accompanied by a large negative shift in the reduction potential (Hildebrandt & Stockburger, 1989a), electron transfer to CCP could occur prior to peroxide binding. However, in the second step of the enzymic cycle (Poulos & Kraut, 1980a), compound I could facilitate its own reduction by inducing a conformational change that converted the bound cyt to a species similar to state II. In this context, it is interesting to note that the crystal structure of compound I reveals movement of loop 175–190 (Edwards et al., 1987), which is part of the proposed cyt binding domain.

Finally, it has been proposed that the conformation of the vinyl substituents of b-type hemes plays an important role in controlling the reduction potential of the heme (Reid et al., 1986). Therefore, it may be of biological significance that cyt(Y) binding, in particular, fixes the position of these substituents more rigidly in the protein matrix of CCP, thereby assuring more rigid control of the enzyme's reduction potential.

Acknowledgments

We are grateful to Dr. M. Stockburger and Professor A. Weller for allowing us to carry out these experiments at the Max-Planck-Institut für Biophysikalische Chemie in Göttingen. We thank Sheryl Nymark and Rita Kohen Avramoglu for purification of the protein samples at Concordia.

Registry No. CCP, 9029-53-2; cyt, 9007-43-6.

References

Abe, M., Kitagawa, T., & Kyogoku, Y. (1978) *J. Chem. Phys. 69*, 4526.

Alshuth, T., & Stockburger, M. (1986) *Photochem. Photobiol. 43*, 55.

Balny, C., Anni, H., & Yonetani, T. (1987) *FEBS Lett. 221*, 349.

Bisson, R., & Capaldi, R. A. (1981) *J. Biol. Chem. 256*, 4362.

Brautigan, D. L., Ferguson-Miller, S., & Margoliash, E. (1978) *Methods Enzymol. 53D*, 131.

Bushnell, G. W., Louis, G. V., & Brayer, G. D. (1990) *J. Mol. Biol. 214*, 585.

Cartling, B. (1988) *Biological Applications of Raman Spectroscopy* (Spiro, T. G., Ed.) Vol. 3, pp 217–248, Wiley, New York.

Choi, S., & Spiro, T. G. (1983) *J. Am. Chem. Soc. 105*, 3683.

Dasgupta, S., Rousseau, D. L., Anni, H., & Yonetani, T. (1989) *J. Biol. Chem. 264*, 654.

Edwards, S. L., & Poulos, T. L. (1990) *J. Biol. Chem. 264*, 2588.

Edwards, S. L., Xuong, N. H., Hamlin, R. C., & Kraut, J. (1987) *Biochemistry 26*, 1503.

English, A. M., Laberge, M., & Walsh, M. (1986) *Inorg. Chim. Acta 123*, 113.
Erman, J. E., & Vitello, L. B. (1980) *J. Biol. Chem. 255*, 6224.
Finzel, B. C., Poulos, T. L., & Kraut, J. (1984) *J. Biol. Chem. 259*, 13027.
Gao, Y., Boyd, J., Williams, R. J. P., & Pielak, G. J. (1990) *Biochemistry 29*, 6994.
Gupta, R. K., & Yonetani, T. (1973) *Biochim. Biophys. Acta 292*, 502.
Hake, R., Zhang, Q., Marohn, J., McLendon, G., & Corin, A. (1991) *Mol. Cryst. Liq. Cryst. 194*, 351.
Hashimoto, S., Teraoka, J., Inubushi, T., Yonetani, T., & Kitagawa, T., (1986) *J. Biol. Chem. 261*, 11110.
Hildebrandt, P. (1990) *Biochim. Biophys. Acta 1040*, 175.
Hildebrandt, P., & Stockburger, M. (1989a) *Biochemistry 28*, 6710.
Hildebrandt, P., & Stockburger, M. (1989b) *Biochemistry 28*, 6722.
Hildebrandt, P., Garda, H., Stier, A., Bachmanova, G. I., Kanaeva, I. P., & Archakov, A. I. (1989) *Eur. J. Biochem. 186*, 383.
Hildebrandt, P., Heimburg, T., & Marsh, D. (1990a) *Eur. Biophys. J. 18*, 193.
Hildebrandt, P., Heimburg, T., Marsh, D., & Powell, G. L. (1990b) *Biochemistry 29*, 1661.
Hoth, L. R., & Erman, J. E. (1984) *Biochim. Biophys. Acta 788*, 151.
Kitagawa, T., & Ozuki, Y. (1987) *Struct. Bonding (Berlin) 64*, 71.
Kornblatt, J. A., & English, A. M. (1986) *Eur. J. Biochem. 155*, 505.
Louie, G. V., & Brayer, G. D. (1990) *J. Mol. Biol. 214*, 527.
Louie, G. V., Hutcheon, W. L. B., & Brayer, G. D. (1988) *J. Mol. Biol. 199*, 252.
Lum, V. R., Brayer, G. D., Louie, G. V., Smith, M., & Mauk, A. G. (1987) *Protein Structure, Folding, and Design 2* (Oxender, D. L., Ed.) pp 143–150, Alan R. Liss, New York.
Margoliash, E., & Bosshard, H. R. (1983) *Trends Biochem. Sci. 8*, 316.
Morikis, D., Li, P., Bangcharoengpaurporg, O., Sage, T. P., & Champion, P. M. (1991) *J. Phys. Chem. 95*, 3391.
Nocek, J. M., Stemp, E. D. A., Finnegan, M. G., Koshy, T. I., Johnson, M. K., Margoliash, E., Mauk, A. G., Smith, M., & Hoffman, B. M. (1991) *J. Am. Chem. Soc. 113*, 6822.
Northrup, S. H., Boles, J. O., & Reynolds, J. C. L. (1988) *Science 241*, 67.
Parthasarathi, N., Hansen, C., Yamaguchi, S., & Spiro, T. G. (1987) *J. Am. Chem. Soc. 109*, 3865.
Pettigrew, G. W. (1978) *FEBS Lett. 86*, 14.
Poulos, T. L., & Kraut, J. (1980a) *J. Biol. Chem. 255*, 8199.
Poulos, T. L., & Kraut, J. (1980b) *J. Biol. Chem. 255*, 10322.
Poulos, T. L., & Finzel, B. C. (1984) *Pept. Protein Rev. 4*, 115.
Poulos, T. L., Freer, S. T., Alden, R. A., Edwards, S. L., Skogland, U., Takio, K., Eriksson, B., Xuong, N. H., Yonetani, T., & Kraut, J. (1980) *J. Biol. Chem. 255*, 575.
Poulos, T. L., Sheriff, S., & Howard, A. J. (1987) *J. Biol. Chem. 263*, 10541.
Reid, L. S., Lim, A. R., & Mauk, A. G. (1986) *J. Am. Chem. Soc. 108*, 8197.
Rönnberg, M., Österlund, K., & Ellfolk, N. (1980) *Biochim. Biophys. Acta 626*, 23.
Rousseau, D. L. (1981) *J. Raman Spectrosc. 10*, 94.
Satterlee, J. D., Moench, S. J., & Erman, J. E. (1987) *Biochim. Biophys. Acta 912*, 87.
Sievers, G., Österlund, K., & Ellfolk, N. (1979) *Biochim. Biophys. Acta 581*, 1.
Smulevich, G., Mauro, J. M., Fishel, L. A., English, A. M., Kraut, J., & Spiro, T. G. (1988) *Biochemistry 27*, 5477.
Smulevich, G., Mantini, A. R., English, A. M., & Mauro, J. M. (1989) *Biochemistry 28*, 5058.
Smulevich, G., Wang, Y., Edwards, S. L., Poulos, T. L., English, A. M., & Spiro, T. G. (1990a) *Biochemistry 29*, 2586.
Smulevich, G., Wang, Y., Mauro, J. M., Wang, J., Fishel, L. A., Kraut, J., & Spiro, Y. G. (1990b) *Biochemistry 29*, 7174.
Smulevich, G., Miller, M. A., Kraut, J., & Spiro, T. G. (1991) *Biochemistry 30*, 9546.
Spiro, T. G., & Li, X.-Y. (1988) *Biological Applications of Raman Spectroscopy* (Spiro, T. G., Ed.) Vol. 3, pp 1–38, Wiley, New York.
Spiro, T. G., Smulevich, G., & Su, C. (1990) *Biochemistry 29*, 4497.
Takano, T., & Dickerson, R. E. (1980) *Proc. Natl. Acad. Sci. U.S.A. 77*, 6371.
Uchida, K., Susai, Y., Hirotani, E., Kimura, T., Yoneya, T., Takeuchi, H., & Harada, I. (1988) *J. Biochem. (Tokyo) 103*, 979.
Valance, W. G., & Strekas, T. C. (1982) *J. Phys. Chem. 86*, 1804.
Vitello, L. R., & Erman, J. E. (1987) *Arch. Biochem. Biophys. 258*, 621.
Waldemeyer, B., Bechtold, R., Bosshard, H. R., & Poulos, T. L. (1982) *J. Biol. Chem. 257*, 6073.
Wang, J., Mauro, J. M., Edwards, S. L., Oatley, S. J., Fishel, L. A., Ashford, V. A., Xuong, N.-H., & Kraut, J. (1990) *Biochemistry 29*, 7160.
Yonetani, T. (1976) *The Enzymes* (Boyer, P. D., Ed.) Vol. 13, pp 345–361, Academic Press, New York.
Yonetani, T., & Anni, H. (1987) *J. Biol. Chem. 262*, 9547.
Zhang, Q., Marohn, J., & McLendon, G. (1990) *J. Phys. Chem. 94*, 8628.